International Journal of Solids and Structures 48 (2011) 2393–2401

Contents lists available at ScienceDirect

International Journal of Solids and Structures

journal homepage: www.elsevier.com/locate/ijsolstr

Magneto-electro-elastic coated inclusion problem and its application to magnetic-piezoelectric composite materials

F. Dinzart *, H. Sabar

Laboratoire de Biomécanique Polymères et Structures, Ecole Nationale d'Ingénieurs de Metz, 1 route d'Ars Laqueny, 57078 Metz Cedex 3, France

ARTICLE INFO

Article history:
Received 14 January 2011
Received in revised form 5 April 2011
Available online 24 April 2011

Keywords:
Micro-mechanics
Magnetic-piezoelectric composite materials
Coated inclusion
Mori–Tanaka's model

ABSTRACT

In this work, a micromechanical model for the estimate of the magneto-electro-elastic behavior of the magnetic-piezoelectric composites with coated reinforcements is proposed. The coating is considered as a thin layer with properties different from those of the inclusion and the matrix. The micromechanical approach based on the Green's functions techniques and on the interfacial operators is designed for solving the magneto-electro-elastic inhomogeneous coated inclusion problem. The effective magneto-electro-elastic properties of the composite containing thinly coated inclusions are obtained through the Mori–Tanaka's model. Numerical investigations into magneto-electro-elastic moduli responsible for the magneto-electric coupling are presented as functions of the volume fraction and characteristics of the coated inclusions. Comparisons with existing models are presented for various shape and orientation of the coated inclusions.

1. Introduction

Consecutively to their attractive applications in smart and adaptative systems using their magneto-electro-mechanical energy conversion capacities, the study of such dedicated 'magneto-electro-elastic' materials has become more extensive in recent years. The coupled phenomena like piezoelectricity and piezomagneticity can be found in some natural single crystals (Alshits et al., 1992) and more widely in specifically dedicated composites (Harshe et al., 1993). The prediction of the overall properties of 'magneto-electric-elastic' composites has aroused great interest among researchers, in particular in the description of the coupled phenomena induced from discontinuous reinforcements. A better understanding of the interaction of microstructures and coupling effects such as magnetolectricity is essential for the comprehensive design of novel materials for desired applications. The magneto-electric (ME) coupling effects result from cross or product properties which are absent from each phases of the composite as described by the Nan et al. (2008) in their review.

The concept of hybrid fiber constituted of a core surrounded by a high performance piezoelectric materials has appeared recently for the sake of improvement of electroelastic properties (Torah et al., 2004). Xie et al. (2008) synthesized hybrid multiferroic $CoFe_2O_4$-$Pb(Zr_{0.52}Ti_{0.4})O_3$ nanofibers by electrospinning and obtained good ferroelectric and ferromagnetic properties measured by piezoresponse force microscopy. The effective properties of a composite are highly affected by the magneto-electro-elastic characteristics and the geometry of the interphase between the constituents. Consequently, studying the influence of a coating layer in 'magneto-electric-elastic' composites may be valuable to better understand the transmission of mechanical, electrical and magnetic fields throughout the inclusion toward the matrix for the sake of improvement of the strength and/or the ME. The increase of the strength may be obtained for example via the introduction of a stiff interphase of defined thickness as demonstrated by Kari et al. (2008) for elastic composites. The ME enhancement is more tricky as it implies coupled mechanical, electrical and magnetic properties. The voluntary introduction of an active interphase (in the sense of the ME) allows to comprehend the transmission of the different fields from the core towards the matrix. A parametric analysis conducted in a further publication may also provide the better material combination for core, coating and matrix to enhance the ME coupling. An interphase layer may be also introduced to model the debonding between the particles and the matrix (Sevostianov and Kachanov, 2007) or to describe hybrid magneto-electric composites synthesized with a core–shell (Islam et al., 2008).

First attempts to model the ME in multilayered composites were restricted to simplified material behavior (Harshe et al., 1993) or to particular geometry: fibrous (Benveniste, 1995) or lamellar composites (Huang et al., 1998). Huang and Kuo (1997) generalized the classical method based on inclusion formulation and Huang et al. (1998) extended the resolution to various shape inclusions thanks to the extension of the classical Eshelby's elastic tensor to magneto-electric behavior. The Green's functions techniques allowed the ME analysis via various homogenization scheme (Mori–Tanaka, self-consistent...), for multi-inclusion and

* Corresponding author. Fax: +33 3 87 34 42 78.
E-mail address: dinzart@enim.fr (F. Dinzart).

0020-7683/$ - see front matter © 2011 Elsevier Ltd. All rights reserved.
doi:10.1016/j.ijsolstr.2011.04.010

inhomogeneity problems (Li, 2000a,b). Among the numerous methods dedicated to overcome the mathematical difficulties induced by the intrinsic electro-mechanical and magneto-mechanical couplings, the finite element technique succeeded to characterize the optimization of the ME in laminate (Liu et al., 2003) or fibrous composites (Lee et al., 2005). The concept of periodic structure was improved by Tang and Yu (2008) via a variational asymptotic homogenization scheme for composites including piezoelectric and magnetoelecric phases both embedded in an epoxy matrix.

The most recent studies dealing with the influence of the interphase properties were conducted in electro-elasticity (Jiang and Cheung, 2001 and Sudak, 2003) and in magneto-electro-elasticity (Shen, 2008 and Tong et al., 2008). They provided exact and analytical results based on the complex variable method in particular configurations (in-plane or anti-plane loading) limiting the implied material properties and the geometry of the reinforcement (essentially cylindrical). To our knowledge, only Li (2000a) proposed a solution to the multi-inclusion and inhomogeneity problems for magneto-electro-elastic composites by extending the double inclusion method developed by Hori and Nemat-Nasser (1993) to equivalent multi-inclusion. The double inclusion method gives the exact solution to the multi-inclusion problem provided that the magneto-electro-elastic fields are uniform in every coating. Generally, these fields are heterogeneous as they are intended to accommodate the incompatible fields between the inclusion, the interphase and the matrix. In the double inclusion model, these complex interactions between the phases are not completely taken into account inducing some imprecision on the effective properties. We propose a method where heterogeneous fields may be considered in the coating.

This work is devoted to the determination of the effective magneto-electro-elastic behavior of a magneto-electro-elastic composite with coated reinforcements in the general case of anisotropic behavior. The thinly coated inclusion is described by two non-homothetic concentric ellipsoidal inclusions. The concept of the interfacial operators initially developed by Hill (1983) in elasticity is widened in magneto-electro-elasticity by the formulation of magneto-electro-elastic interfacial operators. By basing itself simultaneously on the Green's functions techniques and the magneto-electro-elastic interfacial operators, this study establishes a new integral equation taking into account the presence of the coating situated between the inclusion and the matrix. This approach has already proved to be effective in the particular cases of elastic (Cherkaoui et al., 1995) and thermo-elastic composites (Cherkaoui et al., 1996) and piezoelectric composites (Dinzart and Sabar, 2009). The formulation of the integral equation and the solution of the magneto-piezoelectric coated inclusion problem are presented in the second section. The effective magneto-electro-elastic moduli of the composite with coated reinforcements are expressed in the third section via a Mori–Tanaka's scheme of homogenization. Applications are conducted for reinforced magneto-electric-elastic composites. Some connections with the double-inclusion model developed by Li (2000a) for magneto-electro-elastic composites are proposed in the particular problem of fibrous composites. The effects of the shape, orientation and volume fraction of the coated inclusions are explored to identify the possible optimization of the ME coupling in magneto-electro-elastic composite with coated reinforcements.

2. Micromechanical approach of the magneto-electro-elastic coated inclusion problem

The topology of the magneto-electro-elastic coated inclusion problem drawn in Fig. 1 is described by an inclusion of volume V_I surrounded by a thin coating of volume V_c. The coating is bounded at its outer boundary to a surrounding homogeneous material (matrix). Each phase is described by magneto-electro-elastic properties including the elastic moduli C, the piezoelectric and piezomagnetic properties denoted by e and q, the dielectric constants κ, the magnetic permeabilities ξ and the magneto-electric coefficients α. In our analysis, the constituents are linear electroelastic and magnetoelastic. The boundaries are assumed perfectly bonded.

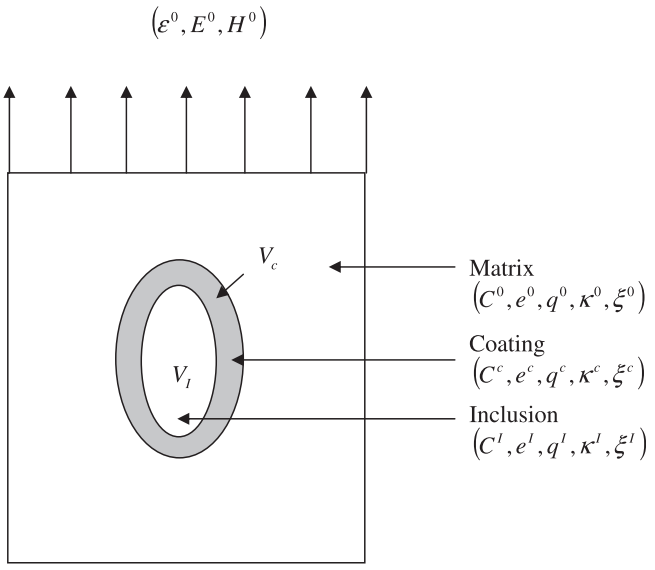

Fig. 1. Topology of the magneto-electro-elastic coated inclusion problem.

2.1. Fundamental equations

For stationary behavior in the absence of free electric and magnetic charges or body forces, the equations of linear magneto-electro-elasticity consist of the constitutive equations, the divergence equations (elastic equilibrium and Gauss' Law), and the gradient equations (strain–displacement, electric field-potential and magnetic field-potential relations). The coupled relationships between the magnetic electric and mechanical variables are given by the following equations:

$$\begin{aligned} \sigma_{ij} &= C_{ijmn}\varepsilon_{mn} - e_{nij}E_n - q_{nij}H_n \\ D_i &= e_{imn}\varepsilon_{mn} + \kappa_{in}E_n + \alpha_{in}H_n \\ B_i &= q_{imn}\varepsilon_{mn} + \alpha_{in}E_n + \xi_{in}H_n \end{aligned} \tag{1}$$

$$\sigma_{ij,j} = 0, \quad D_{i,i} = 0, \quad B_{i,i} = 0 \tag{2}$$

$$\varepsilon_{mn} = \frac{1}{2}(u_{m,n} + u_{n,m}), \quad E_n = -\Phi_{,n}, \quad H_n = -\chi_{,n} \tag{3}$$

σ_{ij}, ε_{mn} and u_n are the elastic stress, strain and displacement. E_n, D_i, and Φ are the electric field, displacement and potential. H_n, B_i, and χ are the magnetic field, flux and potential. The elastic stiffness tensor denoted by C_{ijmn} is measured in constants electric and magnetic fields, the third order tensors e_{jmn} and q_{jmn} are the piezoelectric and piezomagnetic properties measured at a constant strain and the second orders tensors κ_{in} and ξ_{in} are the dielectric and magnetic permeabilities and α_{in} the magneto-electric coefficients.

For the sake of simplification, the coupled interaction between the magnetic, electric and mechanical variables are rewritten by using displacement-magneto-electric potential U, magneto-electro-elastic Z and stress-magneto-electric Σ fields (Alshits et al., 1992):

$$U_M = \begin{cases} u_m \\ \Phi \\ \zeta \end{cases}, \quad Z_{Mn} = \begin{cases} \varepsilon_{mn} \\ -E_n \\ -H_n \end{cases}, \quad \Sigma_{nM} = \begin{cases} \sigma_{nm} \\ D_n \\ B_n \end{cases} \quad \text{with} \quad \begin{cases} M = 1,2,3 \\ M = 4 \\ M = 5 \end{cases} \tag{4}$$

The magneto-electro-elastic moduli L are expressed as:

$$L_{ijMn} = \begin{bmatrix} C_{ijmn} & e_{ijn} & q_{ijn} \\ e_{imn} & -\kappa_{in} & -\alpha_{in} \\ q_{imn} & -\alpha_{in} & -\xi_{in} \end{bmatrix} \quad \text{with} \quad \begin{bmatrix} J,M = 1,2,3 & J = 1,2,3\ M = 4 & J = 1,2,3\ M = 5 \\ M = 1,2,3\ J = 4 & J = 4\ M = 4 & J = 4\ M = 5 \\ M = 1,2,3\ J = 4 & J = 5\ M = 4 & J = 5\ M = 5 \end{bmatrix} \tag{5}$$

with the index (J,M) defined for the same position of the matrix L.

The symmetry properties of L_{ijMn} are induced from those of C_{ijmn}, e_{ijn} and q_{ijn}. The coupled magneto-electro-elastic behavior can be rewritten into the single shorthand equation:

$$\Sigma_{ij} = L_{ijMn} Z_{Mn} \tag{6}$$

Introducing this equation in shorthand notations of (4) and (6), we obtain the equilibrium equations for the magneto-electro-elastic potential field U_M for given boundary conditions:

$$(L_{ijMn} U_{M,n})_{,i} = 0 \tag{7}$$

2.2. Integral equation

The problem consists of finding U_M, Z_{Mn} and Σ_{ij} at an arbitrary point r located in each phase when the magneto-electro-elastic material is loaded by homogeneous boundary conditions $U_M^0 = Z_{Mn}^0 x_n$ where Z_{Mn}^0 is an uniform field. Using de Green's functions techniques $\mathbf{G}_{JK}(r)$, we transform the differential Eq. (7) into an integral equation linking the magneto-electro-elastic field Z_{Kl} with the tensor Z_{Kl}^0:

$$Z_{Kl}(r) = Z_{Kl}^0 - \int_{V'} \Gamma_{ijKl}(r - r') \delta L_{ijMn}(r') Z_{Mn}(r') dV' \tag{8}$$

where V is the volume of the infinite medium and $\Gamma(r - r')$ is the magneto-electro-elastic modified Green's tensor of the reference medium L^0 defined by $\Gamma_{ijKl}(r - r') = -\mathbf{G}_{JK,il}(r - r')$ The local magneto-electro-elastic tensor $L(r)$ can be splitted into a uniform part L^0 of the infinite homogeneous medium and the fluctuating part $\delta L(r)$ due to the inhomogeneous coated inclusion:

$$L(r) = L^0 + \delta L(r) \tag{9}$$

As the inclusion and the thin surrounding coating are characterized by their magneto-electro-elastic moduli L^I and L^c of volume V_I and V_c, the heterogeneous part $\delta L(r)$ may be expressed as:

$$\delta L(r) = \Delta L^I \theta^I(r) + \Delta L^c \theta^c(r) \tag{11}$$

where $\Delta L^I = L^I - L^0$ and $\Delta L^c = L^c - L^0$.

$\theta^I(r)$ and $\theta^c(r)$ are the Heaviside step functions defined by:

$$\theta^I(r) = \begin{cases} 1 & \text{if } r \in V_I \\ 0 & \text{if } r \notin V_I \end{cases}, \quad \theta^2(r) = \begin{cases} 1 & \text{if } r \in V_2 \\ 0 & \text{if } r \notin V_2 \end{cases}, \quad \theta^c(r) = \theta^2(r) - \theta^I(r) \tag{12}$$

In this case, V_2 denotes the volume of the composite inclusion ($V_2 = V_I \cup V_c$).

Substituting (11) in (8) and using the properties (12) of $\theta^I(r)$ and $\theta^c(r)$, we obtain:

$$Z_{Kl}(r) = Z_{Kl}^0 - \int_{V_I'} \Gamma_{ijKl}(r - r') \Delta L_{ijMn}^I(r') Z_{Mn}(r') dV' - \int_{V_c'} \Gamma_{ijKl}(r - r') \Delta L_{ijMn}^c(r') Z_{Mn}(r') dV' \tag{13}$$

As $L(r)$ is quite uniform by pieces, we consider averaged values of the fields of each phase: $\overline{Z}^I$, $\overline{Z}^c$ and $\overline{Z}^2$ in the inclusion, the coating and the composite inclusion respectively:

$$\overline{Z}_{Mn}^I = \frac{1}{V_I} \int_{V_I} Z_{Mn}(r) dV, \quad \overline{Z}_{Mn}^c = \frac{1}{V_c} \int_{V_c} Z_{Mn}(r) dV,$$
$$\overline{Z}_{Mn}^2 = \frac{1}{V_2} \int_{V_2} Z_{Mn}(r) dV \tag{14}$$

The field $\overline{Z}^2$ over the composite inclusion is issued from averaging of (13):

$$\overline{Z}_{Kl}^2 = Z_{Kl}^0 - \frac{1}{V_2} \int_{V_2} \int_{V_I'} \Gamma_{ijKl}(r - r') \Delta L_{ijMn}^I(r') Z_{Mn}(r') dV' dV - \frac{1}{V_2} \int_{V_2} \int_{V_c'} \Gamma_{ijKl}(r - r') \Delta L_{ijMn}^c(r') Z_{Mn}(r') dV' dV \tag{15}$$

With use of the uniform Eshelby's magneto-electro-elastic tensor $T^2(L^0)$ defined as $\int_{V_2} \Gamma(r - r') dV = T^2(L^0)$ if $r' \in V_2$ (see Eshelby, 1957 and Li and Dunn, 1998), the field $\overline{Z}^2$ may be expressed as by considering (14):

$$\overline{Z}_{Kl}^2 = Z_{Kl}^0 - \frac{V_I}{V_2} T_{ijKl}^2(L^0) \Delta L_{ijMn}^I \overline{Z}_{Mn}^I - \frac{V_c}{V_2} T_{ijKl}^2(L^0) \Delta L_{ijMn}^c \overline{Z}_{Mn}^c \tag{16}$$

As $\overline{Z}_{Kl}^2 = \frac{V_I}{V_2} \overline{Z}_{Kl}^I + \frac{V_c}{V_2} \overline{Z}_{Kl}^c$, we obtain:

$$\frac{V_I}{V_2} \left(I_{KlMn} + T_{ijKl}^2(L^0) \Delta L_{ijMn}^I \right) \overline{Z}_{Mn}^I + \frac{V_c}{V_2} \left(I_{KlMn} + T_{ijKl}^2(L^0) \Delta L_{ijMn}^c \right) \overline{Z}_{Mn}^c = Z_{Kl}^0 \tag{17}$$

where I is the notation for the fourth order and two second order identity tensors:

$$I_{KlMn} = \begin{bmatrix} (\delta_{km}\delta_{ln} + \delta_{kn}\delta_{lm})/2 & 0 & 0 \\ 0 & \delta_{nl} & 0 \\ 0 & 0 & \delta_{nl} \end{bmatrix}$$
$$\text{with} \quad \begin{bmatrix} K,M = 1,2,3 & K = 1,2,3\ M = 4 & K = 1,2,3\ M = 5 \\ M = 1,2,3\ K = 4 & K = 4\ M = 4 & K = 4\ M = 5 \\ M = 1,2,3\ K = 4 & K = 5\ M = 4 & K = 5\ M = 5 \end{bmatrix} \tag{18}$$

The index (K,M) are defined for the same position of the matrix I.

The remaining unknowns are then $\overline{Z}^I$ and $\overline{Z}^c$ which have to be related by an additional equation introduced in the following section with use of magneto-electro-elastic interfacial operators.

2.3. Magneto-electro-elastic interfacial operators

We consider an interface between two homogeneous magneto-electro-elastic medium made of two different phases whose magneto-electro-elastic moduli are denoted by L^+ and L^-. In the context of continuum mechanics, the interface is modeled by a mathematical surface across which material properties change discontinuously. As presented by Mura (1987) in his description of the discontinuities throughout interfacial surfaces and developed by Hill (1983) also in elasticity, by Dunn (1994) and Dunn and Taya (1994) in piezoelectricity, the stress–strain magneto-electric fields are discontinuous across the interface and their jumps are related by the interfacial operators. This concept is widened in this work to the case of a magneto-electro-elastic behavior. Under perfect bonding hypothesis, the continuity of the magneto-electro-elastic potential, the interfacial tension and the electric displacement and magnetic displacement across the interface are expressed:

$$[U_M] = U_M^+ - U_M^- = 0 \tag{19}$$

$$[\Sigma_{ij}] N_J = \left(\Sigma_{ij}^+ - \Sigma_{ij}^- \right) N_J = 0 \tag{20}$$

where a normal unit vector N is given by

$$N_J = \begin{cases} n_j & J = 1,2,3 \\ 1 & J = 4 \\ 1 & J = 5 \end{cases} \quad (21)$$

with n_i the outward unit normal of the interface directed of $(-)$ towards $(+)$.

At an arbitrary point r of the interface, the compatibility conditions $du_i = u_{i,j}dx_j$, $d\Phi = \Phi_j dx_j$ and $d\chi = \chi_j dx_j$ added to the continuity of displacement and potential along the boundary impose the relations: $[u_{i,j}]dx_j = 0$, $[\Phi_j]dx_j = 0$ and $[\chi_j]dx_j = 0$. Since $n_j dx_j = 0$, the displacement and potentials gradient are proportional to the unit normal $[u_{i,j}] = \lambda_i n_j$, $[\Phi_j] = \lambda_E n_j$ and $[\chi_j] = \lambda_H n_j$ where λ_i, λ_E and λ_H are the proportionality vector and scalars.

The magneto-electro-elastic displacement jump is expressed as:

$$[Z_{Mn}] = \lambda_M N_N \quad (22)$$

where the magnitude of the jump λ_M is defined by

$$\lambda_M = \begin{cases} \lambda_m & M = 1,2,3 \\ -\lambda_E & M = 4 \\ -\lambda_H & M = 5 \end{cases} \quad (23)$$

The continuity condition (20) induces $\left(L^+_{ijMn}Z^+_{Mn} - L^-_{ijMn}Z^-_{Mn}\right)N_j = 0$. After introduction of the Christoffel's matrix $K^*(^* = {}^+ or {}^-)$ defined by $K^*_{iM} = L^*_{ijMn}N_J N_N$, the magneto-electro-elastic jump λ_M may be evaluated in terms of the magneto-electro-elastic field on both sides of the interface. Under the specified coated inclusion problem, the phase $(-)$ is the inclusion surrounded by the coating of phase $(+)$. Thus, the fields $Z^I(r^-)$ inside the inclusion and $Z^c(r^+)$ inside the coating in the neighborhood of the interface may be related via an magneto-electro-elastic interfacial operator P (for more precision see Dinzart and Sabar (2009) in the case of electro-elasticity:

$$Z^c_{Mn}(r^+) = Z^I_{Mn}(r^-) + P^c_{ijMn}(L^c, N)\Delta L^{Ic}_{ijRs}Z^I_{Rs}(r^-) \quad (24)$$

where P^c is defined as function of the Christoffel's matrix K by

$$P^c_{ijMn}(L^c, N) = \frac{1}{4}\left(K^{c^{-1}}_{iM}N_J N_N + K^{c^{-1}}_{jM}N_I N_N + K^{c^{-1}}_{iN}N_J N_M + K^{c^{-1}}_{jN}N_I N_M\right).$$

2.4. Average magneto-electro-elastic field inside the inclusion and the coating

To establish the localization formulae between the average field in each phase and the macroscopic field Z^0, the field $Z^I(r^-)$ is replaced by its average value $\overline{Z}^I$ over the inclusion. So, the Eq. (24) becomes:

$$Z^c_{Mn}(r^+) = \overline{Z}^I_{Mn} + P^c_{ijMn}(L^c, N)\Delta L^{Ic}_{ijRs}\overline{Z}^I_{Rs} \quad (25)$$

Under the thin coating assumption, the mean value of the field in the coating is obtained by considering that $Z^c(r^+)$ depends only on the boundary's normal of V_I, which leads to:

$$\overline{Z}^c_{Mn} = \overline{Z}^I_{Mn} + T^c_{IJMn}(L^c)\Delta L^{Ic}_{ijRs}\overline{Z}^I_{Rs} \quad \text{with}$$
$$T^c_{IJMn}(L^c) = \frac{1}{V_c}\int_{V_c} P^c_{ijMn}(L^c, N)dV \quad (26)$$

The problem of localization for the magneto-electro-elastic coated inclusion is solved by supplying the fields within the inclusion and the coating as function of the macroscopic uniform field in the following system:

$$\begin{cases} \frac{V_I}{V_2}\left(I_{KlMn} + T^2_{rSKl}(L^0)\Delta L^I_{rSMn}\right)\overline{Z}^I_{Mn} + \frac{V_c}{V_2}\left(I_{KlMn} + T^2_{rSKl}(L^0)\Delta L^c_{rSMn}\right)\overline{Z}^c_{Mn} = Z^0_{Kl} \\ Z^c_{Kl} = Z^I_{Kl} + T^c_{rSKl}(L^c)\Delta L^{Ic}_{rSMn}Z^I_{Mn} \end{cases} \quad (27)$$

The resolution requires the knowledge of tensors T^2 and T^c. The tensor T^c can be expressed as Dinzart and Sabar (2009):

$$T^c_{ijKl}(L^c) = T^I_{ijKl}(L^c) - \frac{V_I}{V_c}\left(T^2_{ijKl}(L^c) - T^I_{ijKl}(L^c)\right) \quad (28)$$

where T^I and T^2 are related respectively to the inclusion V_I and the composite inclusion V_2. In the case of ellipsoidal inclusions and of anisotropic tensors L^0, T^I and T^2 are obtained via a numeric method using the Fourier transformation of the Green's tensor. Numeric algorithm intended to estimate the tensors T^I and T^2 was developed by Li (2000a). The Eshelby's tensors are a function of the magneto-electro-elastic moduli of the reference medium and of the shape and the orientation of the inclusions. The analysis is conducted by following the scheme described in the previous section leading to the determination of the magneto-electro-elastic Eshelby's tensors T^2 and T^I which last can be considered as $T^I = T^2$ in the homothetic topology of coated inclusion.

In the next part, the previous results are used to predict the effective properties of a composite material made of several coated inclusion in a matrix. The theoretical study is based on the Mori–Tanaka's scheme.

3. Effective magneto-electro-elastic properties of the composite with coated reinforcements

3.1. Mori Tanaka's approach

We assume the material as being a mixture of three phases. The first phase is constituted by several inclusions with magneto-electro-elastic moduli L^I. Each inclusion is surrounding by a thin layer of another phase with magneto-electro-elastic moduli L^c. The coated inclusions are bonded to a matrix whose magneto-electro-elastic moduli are L^M.

When this composite is subjected to homogeneous magneto-electro-elastic boundary conditions $U^0_M = Z^0_{Mn}x_n$ it gives rise to internal strain and stress, electric and magnetic fields in the composite, whose averages, over the representative volume element, are denoted by $\overline{Z}$ and $\overline{\Sigma}$ respectively, so that:

$$\overline{Z}_{Mn} = \frac{1}{V}\int_V Z_{Mn}(r)dV, \quad \overline{\Sigma}_{ij} = \frac{1}{V}\int_V \Sigma_{ij}(r)dV \quad (29)$$

These averages serve to define the effective magneto-electro-elastic properties L^{eff} of a composite according to the relation:

$$\overline{\Sigma}_{iJ} = L^{eff}_{ijMn}\overline{Z}_{Mn} \quad (30)$$

On the other hand, it can be written from the linearity of the problem that:

$$\overline{Z}^I_{Mn} = A^I_{MnKl}\overline{Z}_{Kl}, \quad \overline{Z}^c_{Mn} = A^c_{MnKl}\overline{Z}_{Kl} \quad (31)$$

where A^I and A^c are the magneto-electro-elastic concentration tensors of the inclusion and the coating respectively. With the help of (29)–(31), the following expression is obtained:

$$L^{eff}_{ijKl} = L^M_{ijKl} + f_I\left(L^I_{ijMn} - L^M_{ijMn}\right)A^I_{MnKl} + f_c\left(L^c_{ijMn} - L^M_{ijMn}\right)A^c_{MnKl} \quad (32)$$

where f_I and f_c denote the volume fraction of the inclusion and the coating respectively. It is seen that the determination of L^{eff} requires only the evaluation of A^I and A^c.

These tensors are calculated by the Mori–Tanaka's method (Mori and Tanaka, 1973) where a single coated inclusion is embedded in a matrix with magneto-electro-elastic behavior defined by L^M. Consequently, A^I and A^c can be deduced formally from Eq. (27) where L^0 is replaced by L^M, so that:

$$A^I = \left[\frac{f_I}{f_I+f_c}(I+f_M T^2(L^M)\Delta L^I)+\frac{f_c}{f_I+f_c}(I+f_M T^2(L^M)\Delta L^c)(I+T^c(L^M)\Delta L^{Ic})\right]^{-1} \quad (33)$$

$$A^c = [(I+T^c(L^M)\Delta L^{Ic})]A^I \quad (34)$$

with $\Delta L^I = L^I - L^M$, $\Delta L^c = L^c - L^M$, $\Delta L^{Ic} = L^I - L^c$ and $f_M = 1 - f_I - f_c$ the volume fraction of the matrix. For the sake of a better linking with the double-inclusion model developed by Li (2000a), the magneto-electro-elastic concentration tensors of the inclusion and the coating are expressed as $A^{I^{(DI)}} = [I + T^2(L^M)\Delta L^I]^{-1}$ and $A^{c^{(DI)}} = [I + T^2(L^M)\Delta L^c]^{-1}$.

3.2. Applications

We apply the above developed homogenization method to a three phase composite constituted by a core surrounded by a piezoelectric coating of $BaTiO_3$ embedded in a magnetic matrix of $CoFe_2O_4$. As already shown by Torah et al. (2004) and retrieved by Dinzart and Sabar (2009), a global improvement of electro-elastic properties may be obtained by the use of piezoelectric layer surrounding a glassy core. Lin and Sodano (2010) have studied a three phase piezoelectric composite constituted by a carbon fiber surrounded by a piezoelectric material embedded in an epoxy matrix. As a consequence, the proposed micromechanical model is applied to composites made of glassy or carbon reinforcement surrounded by a thin piezoelectric layer embedded in a magnetic matrix. The piezoelectric, magneto-electric and reinforcement phases are both transversely isotropic. The piezoelectric and magneto-electric media present permittivity constants responsible for the electro-mechanical and the magneto-mechanical couplings. These piezoelectric and piezomagnetic constants are denoted (e_{31}, e_{33}, e_{15}) and (q_{31}, q_{33}, q_{15}) respectively by using the Nye (1957) convention: the index ij or kl in the tensors e_{ijk} and q_{ijk} are replaced by m or n when ij or kl take values (1,2,3) and m or n assumes the values (1,2,3,4,5,6). It is thought-worthy that both materials present no magneto-electric coupling leading to parameters α_{11} and α_{33} equals to zero. The constants for the magneto-electric matrix $CoFe_2O_4$, the piezoelectric medium $BaTiO_3$ are provided in Table 1 from Huang and Kuo (1997). The characteristics of the glass of grade E are taken from Saint-Gobain data. The material properties of the carbon core are taken from Odegard (2004). For both these reinforcement materials, the magnetic coefficients ξ_{11} and ξ_{33} are taken small enough but equal to $10^{-6} Ns^2/C^2$ in order to assure the mathematical inversion of the tensors and the magneto-electric properties q_{ijk} are assumed identically equal to zero.

The volume fraction of the coating is a percentage of the inclusion volume fraction and is represented by its normalized thickness $\Delta a/a$ where a is the inclusion radius. Lamellar, spherical or cylindrical fibers are analyzed through a shape factor defined as the ratio c/a where c is the third half axe of inclusion along the poling direction x_3.

We analyze successively the influence of the thickness of the coating, the shape and the orientation effects of the coated inclusion and eventually the consequence of the material choice for the core.

Table 1
Magneto-electro-elastic materials properties.

	$BaTiO_3$	$CoFe_2O_4$	Glass	Carbon
$C_{11}(GPa)$	166	286	88.8	24
$C_{12}(GPa)$	77	173	29.6	9.7
$C_{13}(GPa)$	78	170	29.6	6.7
$C_{33}(GPa)$	162	269.5	88.8	11
$C_{44}(GPa)$	44	45.3	29.6	27
$\kappa_{11}(10^{-9}C^2/Nm^2)$	11.2	0.08	0.056	0.1062
$\kappa_{33}(10^{-9}C^2/Nm^2)$	12.6	0.093	0.056	0.1062
$\xi_{11}(10^{-6}Ns^2/C^2)$	5	−590	1	1
$\xi_{33}(10^{-6}Ns^2/C^2)$	10	157	1	1
$e_{31}(C/m^2)$	−4.4	0	0	0
$e_{33}(C/m^2)$	18.6	0	0	0
$e_{15}(C/m^2)$	11.6	0	0	0
$q_{31}(N/Am)$	0	580.2	0	0
$q_{33}(N/Am)$	0	699.7	0	0
$q_{15}(N/Am)$	0	550	0	0

3.2.1. Influence of the thickness layer

The study is further conducted for a three phase composite made of glass fibrous core surrounded by a thin piezoelectric layer both embedded in a magnetic matrix. The evolution of the ME coupling coefficients α_{11}^{eff} and α_{33}^{eff} are presented for various normalized thickness $\Delta a/a$ taken below 10% in Figs. 2a and 2b. Our results are in good agreement with the effective properties predicted with the double-inclusion scheme formulated by Li (2000a). The similar study we conducted in electro-elasticity (Dinzart and Sabar, 2009) showed differences between our method and the double inclusion scheme in the case of spherical shape. These differences may be explained by the lack of one integral term during the generalization from local eigen-field to average eigen-field of each phase in the double inclusion method (as pointed out by Hu and Weng, 2000). The concordances of our results with the exact results produced by Jiang and Cheung (2001) and Sudak (2003) allowed us to validate our scheme of resolution of the coated inclusion problem.

The ME coupling shows attenuated effects for α_{11}^{eff} and α_{33}^{eff} when compared to the $BaTiO_3/CoFe_2O_4$ fibrous composite (Benveniste, 1995; Tang and Yu, 2008; Li, 2000a) due to the fewer part of piezoelectric material implicated in the coupling phenomena. However, the ME coupling coefficients are greater by increasing the thickness of the coating i.e. the piezoelectric rate. The optimized volume fraction at the extremum of the ME coupling α_{33}^{eff} diminishes from 44% for the $BaTiO_3/CoFe_2O_4$ composite (Tang and Yu, 2008; Zhang and Soh, 2005) to 38% for the Glass/$BaTiO_3/CoFe_2O_4$ hybrid composite. Similar trend may be observed for the coefficient α_{11}^{eff}: the optimized volume fraction varies from 86 % for non-coated fiber to 50%, 53% and 63% for the thickness $\Delta a/a$ equal to 2%, 5% and 10% respectively.

3.2.2. Influence of the shape

The influence of the shape of the reinforcement is conducted for $BaTiO_3/CoFe_2O_4$ composites and for Glass/$BaTiO_3/CoFe_2O_4$ hybrid composites. As already demonstrated by Benveniste (1995) and by Tang and Yu (2008) for fibrous $BaTiO_3/CoFe_2O_4$ composite, the ME coupling α_{33}^{eff} is positive whereas the ME coupling α_{11}^{eff} is

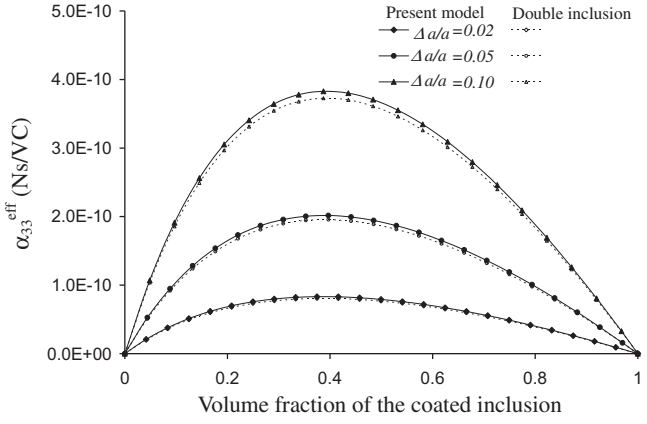

Fig. 2a. Influence of the $BaTiO_3$ coating thickness on the effective ME coupling α_{33}^{eff} for Glass/$BaTiO_3$/ $CoFe_2O_4$ cylindrical composites ($c/a = 100$).

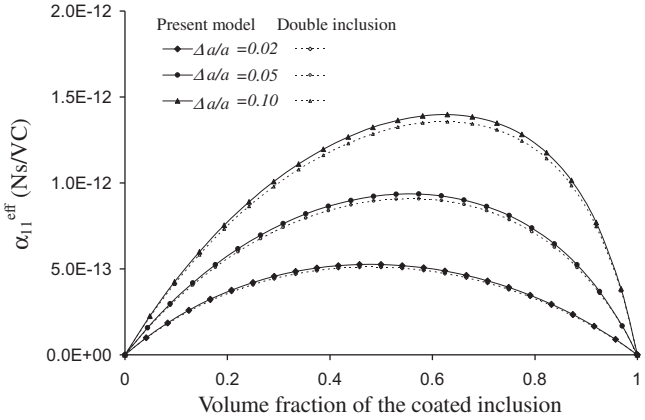

Fig. 2b. Influence of the $BaTiO_3$ coating thickness on the effective ME coupling α_{11}^{eff} for Glass/$BaTiO_3$/ $CoFe_2O_4$ cylindrical composites ($c/a = 100$).

negative consecutively to opposite signs of e_{31} and e_{33} in piezoelectric phase and identical signs of q_{31} and q_{33} in magnetic phase: this induces an offset in interaction between the electric E_3 and magnetic H_3 fields in the poling direction. This phenomenon is inversed for α_{33}^{eff} in the case of spherical or flattened shape (Li, 2000b). Similar trends are observed for Glass/$BaTiO_3$/$CoFe_2O_4$ hybrid composites. The ME coefficient α_{33}^{eff} is first drawn in Fig. 3 for various shape factor c/a at a fixed thickness of the coating $\Delta a/a = 0.02$. The lamellar shape conducts to a decrease of the ME coupling α_{33}^{eff} consecutive to this peculiar shape and to the fewer contribution of the piezoelectric phase in the coating. The spherical shape gives a negative ME coupling α_{33}^{eff} as in $BaTiO_3$/$CoFe_2O_4$ composite (Zhang and Soh, 2005); the minimum of α_{33}^{eff} is shifted towards the smaller volume fraction of the coated inclusion as already described for the cylindrical shape in the previous section. As already observed by Li (2000a), the ME coupling effect α_{33}^{eff} results from the transmission of the stresses σ_{33} and σ_{11} from the piezoelectric phase and from the induced balance with the magnetic flux in the magneto-electric phase. The shear stress σ_{13} gives rise to magnetic flux in the piezoelectric phase and diminishes the α_{11}^{eff} coefficient as the magnetic properties in the piezoelectric phase are three order smaller than in the magneto-electric phase. The lamellar shape leads to highest ME coefficient α_{11}^{eff} since the interactions between piezoelectric and magneto-electric phases are maximized in the orthogonal plane. The discussion of Li (2000a) may be consulted for the complete description of mechanisms implied during the ME coupling.

These observations may be retrieved by analyzing the ME coefficients α_{33}^{eff} and α_{11}^{eff} as function of the aspect ration c/a for $BaTiO_3$/$CoFe_2O_4$ composites (Figs. 4a and 4b) and for Glass/$BaTiO_3$/$CoFe_2O_4$ hybrid composites (Figs. 5a and 5b) for a relative thickness of the coating $\Delta a/a = 0.02$. The plots present different volume fractions f of the inclusion or the coated inclusion from 10% to 50%. In the case of $BaTiO_3$/$CoFe_2O_4$ composite, the ME coefficients present a great evolution when the shape changes from lamellar to fibrous; the range of variation is found between 0.001 to 0.1 for α_{11}^{eff} and between 1 to 100 for α_{33}^{eff}. Similar trends were observed by Srinivas and Li (2005) with a slight shift of the evolution range which may be attributed to a different homogenization scheme, the extremum values of α_{11}^{eff} and α_{33}^{eff} are comparable (respectively $-5.10^{-8} Ns/VC$ and $4.10^{-9} Ns/VC$ for the PZT-5H/$CoFe_2O_4$ composite studied by Srinivas and Li (2005) versus $-3.5.10^{-8} Ns/VC$ and $3.10^{-9} Ns/VC$ for the $BaTiO_3$/$CoFe_2O_4$ composite studied here). However, as seen in Fig. 4a, for intermediate shape factor describing slightly flattened spherical inclusion ($c/a = 0.45$), the ME coefficient α_{33}^{eff} presents a minimum not described by Srinivas and Li (2005). The minimized value of α_{33}^{eff} appears amplified for Glass/$BaTiO_3$/$CoFe_2O_4$ hybrid composite. The combination of the negative and positive magnetic properties ξ_{11} and ξ_{33} for the piezoelectric and magneto-electric phases may favor the existence of extremum values in the resolution (Srinivas and Li considered in their analysis both values ξ_{11} and ξ_{33} positives and identical for each phase). As already observed for the ME coefficient α_{33}^{eff}, the coefficient α_{11}^{eff} presents the same evolution with regards to the aspect factor c/a for the simple $BaTiO_3$/$CoFe_2O_4$ composite and for the hybrid Glass/$BaTiO_3$/$CoFe_2O_4$ composite (Figs. 4b and 5b) with an attenuated values as expected for fewer participation of the piezoelectric phase when used as coating.

A change of sign of the ME coefficient α_{33}^{eff} appears for the same shape factor c/a around 2 (slightly ellipsoidal with the great axe in the poling direction) for $BaTiO_3$/$CoFe_2O_4$ composite (Fig. 4a). This singular shape corresponds to a particular combination of the piezoelectric and piezomagnetic properties as discussed by Li (2000a). Two changes of sign of the ME coefficient α_{33}^{eff} are observed for the Glass/$BaTiO_3$/$CoFe_2O_4$ hybrid composite (Fig. 5a) when the shape evolves from flattened ($c/a \ll 1$) to cylindrical ($c/a \gg 1$): around $c/a \approx 0.06$ and $c/a \approx 4$. The change of sign of the ME coefficient α_{33}^{eff} appears almost independent on the volume fraction: this is due to the proportion of the interacting piezoelectric and piezomagnetic properties which remains quite the same whatever the volume fraction is. The slight scattering in shape factor where

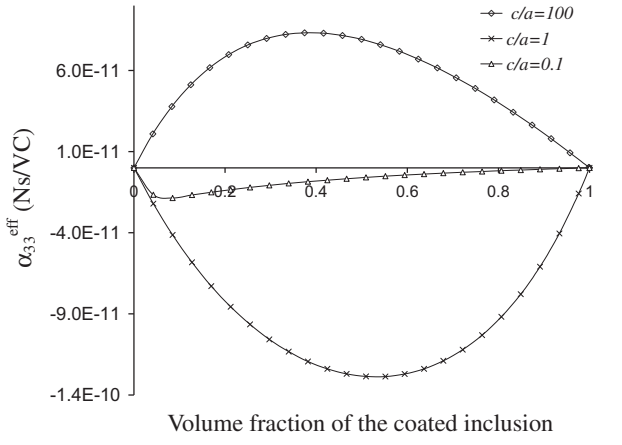

Fig. 3. Influence of the $BaTiO_3$ reinforcement shape on the effective ME coupling α_{33}^{eff} for Glass/$BaTiO_3$/ $CoFe_2O_4$ composites ($\Delta a/a = 0.02$) as function of the volume fraction.

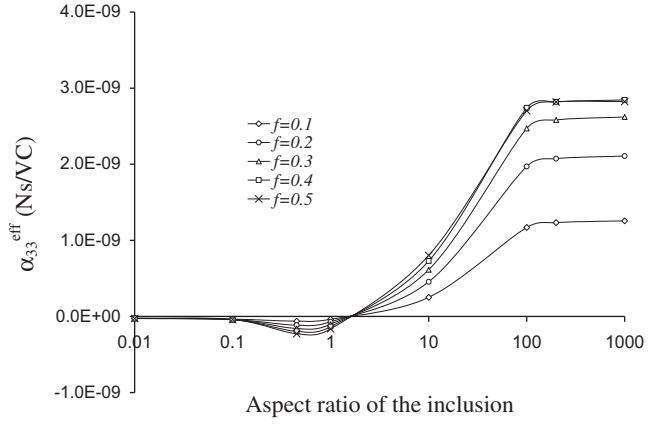

Fig. 4a. Influence of the $BaTiO_3$ reinforcement shape on the effective ME coupling α_{33}^{eff} for $BaTiO_3$/ $CoFe_2O_4$ composites ($\Delta a/a = 0$).

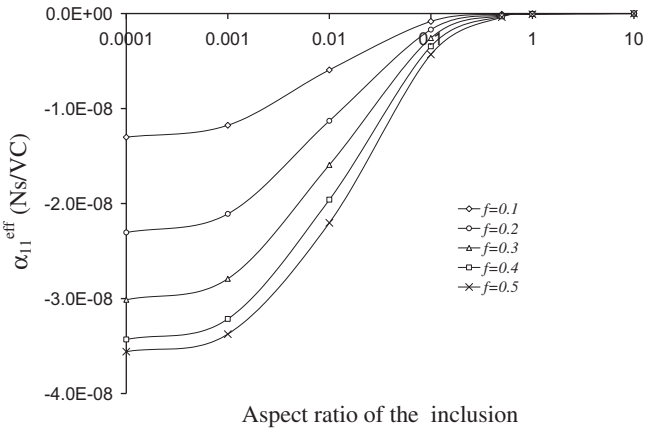

Fig. 4b. Influence of the $BaTiO_3$ reinforcement shape on the effective ME coupling α_{11}^{eff} for $BaTiO_3$/ $CoFe_2O_4$ composites ($\Delta a/a = 0$).

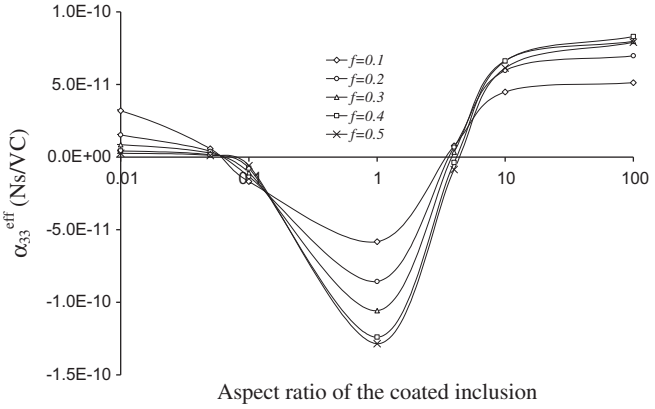

Fig. 5a. Influence of the $BaTiO_3$ reinforcement shape on the effective ME coupling α_{33}^{eff} for Glass/$BaTiO_3$/ $CoFe_2O_4$ composites ($\Delta a/a = 0.02$).

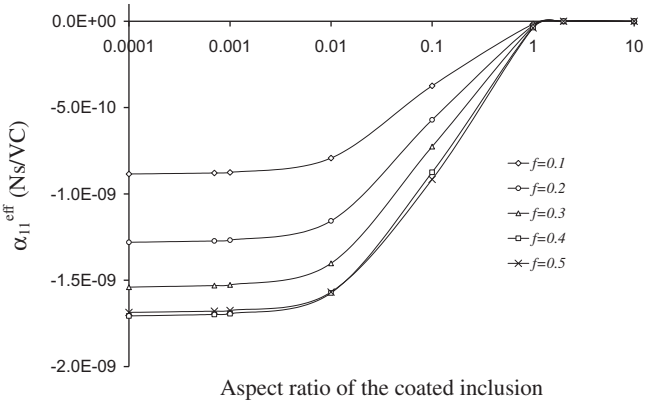

Fig. 5b. Influence of the $BaTiO_3$ reinforcement shape on the effective ME coupling α_{11}^{eff} for Glass/$BaTiO_3$/ $CoFe_2O_4$ composites ($\Delta a/a = 0.02$).

the change of sign occurs in the coated inclusion results from the difference of the repartition of the properties more pronounced in the coating.

3.2.3. Influence of the orientation

We present the influence of the orientation of the fibrous reinforcement in Glass/$BaTiO_3$/$CoFe_2O_4$ fibrous composite. Both core and coating are affected by the orientation described by three Euler angles (θ, ψ, ϕ). This induced anisotropy affects the tensors of second rank κ_{in}, ξ_{in}, of third rank e_{jmn} and q_{jmn}, and of fourth rank C_{ijmn}. The effective second rank tensor α_{in}^{eff} is consequently affected by the orientation effects. The terms of the matrix L_{ijMn} are transformed from their principal value in local coordinate to the global coordinate thanks the direction matrix T defined as:

$$T^{-1} = \begin{bmatrix} \cos\psi\cos\theta\cos\phi - \sin\psi\sin\phi & \sin\psi\cos\theta\cos\phi - \cos\psi\sin\phi & -\sin\theta\cos\phi \\ -\cos\psi\cos\theta\sin\phi - \sin\psi\cos\phi & -\sin\psi\cos\theta\sin\phi - \cos\psi\cos\phi & \sin\theta\sin\phi \\ \sin\theta\cos\psi & \sin\theta\sin\psi & \cos\theta \end{bmatrix} \tag{35}$$

We consider the influence of a single orientation defined by the angle ϕ with the poling direction x_3 on fibrous aligned reinforcement ($c/a = 100$). We only present the influence of the orientation on the ME coefficient α_{33}^{eff} in Fig. 6a for various angle ϕ. The orientation induces a decrease of the inclusion height in the poling direction by a factor $\cos\phi$ which is combined to an increase of the coating surface area in the orthogonal plane by a factor $1/\cos^2\phi$. The balance between these two effects is maximized for the orientation $\phi = 45^\circ$ as may be observed in Fig. 6b which presents the ME coefficient evolution α_{33}^{eff} as function of the orientation for fixed volume fraction of the coated inclusion. The orientation effect may be compared to a flattening of the coated inclusion combined with an increase of the coating thickness whose effects are described above in Fig. 5a.

3.2.4. Influence of the choice of the material core

We further analyze the material choice for the core of the reinforced hybrid composite, the piezoelectric surrounding and the magneto-electric matrix taken identical. The ME coefficient α_{33}^{eff} plotted in Fig. 7a remains positive whatever the chosen core but shows attenuated values when compared to the $BaTiO_3/CoFe_2O_4$ fibrous composite due to the fewer part of piezoelectric material implicated in the coupling phenomena. The ME coupling coefficients are greater for the glass core than for the carbon core: this phenomenon results from the transfer of the elastic strain throughout the phases from the core towards the matrix. As described by Huang et al. (2000), the ME coupling α_{33}^{eff} depends on the elastic moduli of the materials in relation with the growth direction of the phase with respect to the poling direction. Benveniste (1995) gave an expression of the ME coupling α_{33}^{eff} for magneto-electric fibrous composite showing an increase of α_{33}^{eff} for close moduli C_{11} and C_{12} in each phase. The mechanical transfer is all the greater that the effective elastic moduli C_{11}^{eff} and C_{12}^{eff} are close to matrix moduli as shown in the Fig. 7b.

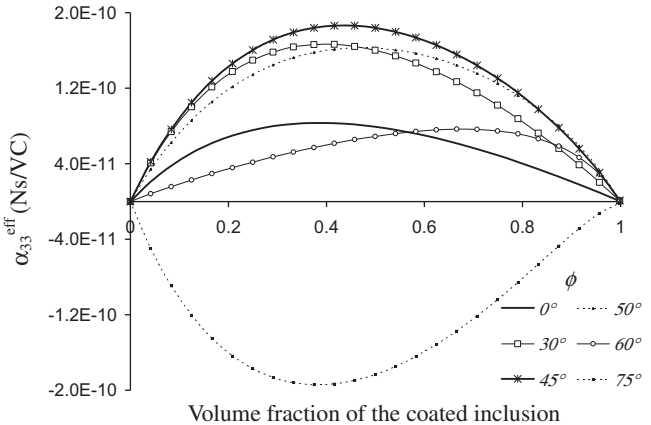

Fig. 6a. Influence of the Glass/$BaTiO_3$ coated fiber orientation on the effective ME coupling α_{33}^{eff} for Glass/$BaTiO_3$/$CoFe_2O_4$ cylindrical composites ($c/a = 100$ and $\Delta a/a = 0.02$) as function of the volume fraction.

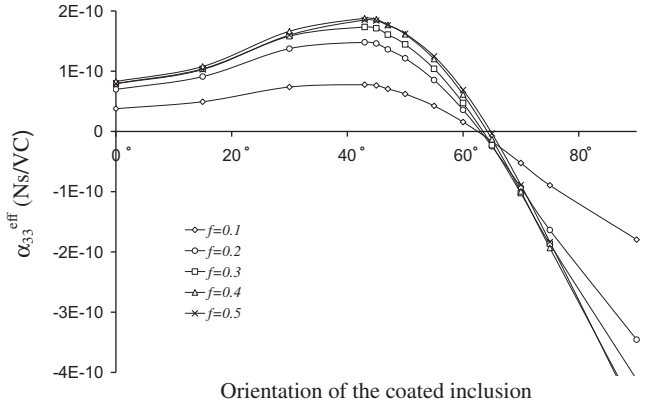

Fig. 6b. Influence of the Glass/$BaTiO_3$ coated fiber orientation on the effective ME coupling α_{33}^{eff} for Glass/$BaTiO_3$/$CoFe_2O_4$ cylindrical composites ($c/a = 100$ and $\Delta a/a = 0.02$).

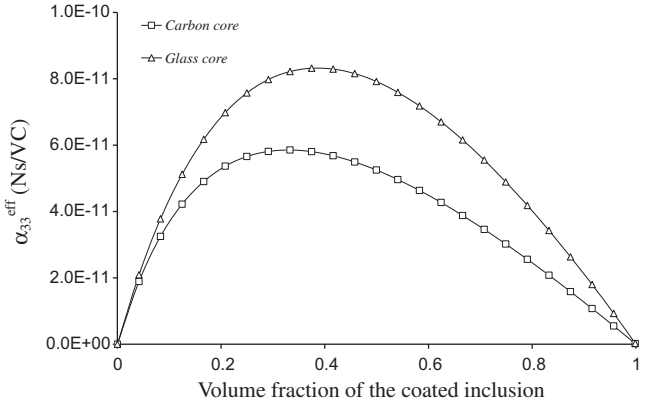

Fig. 7a. Effective ME coupling α_{33}^{eff} for $BaTiO_3$/$CoFe_2O_4$ fibrous composites reinforced by glassy or carbon core fiber ($c/a = 100$ and $\Delta a/a = 0.02$).

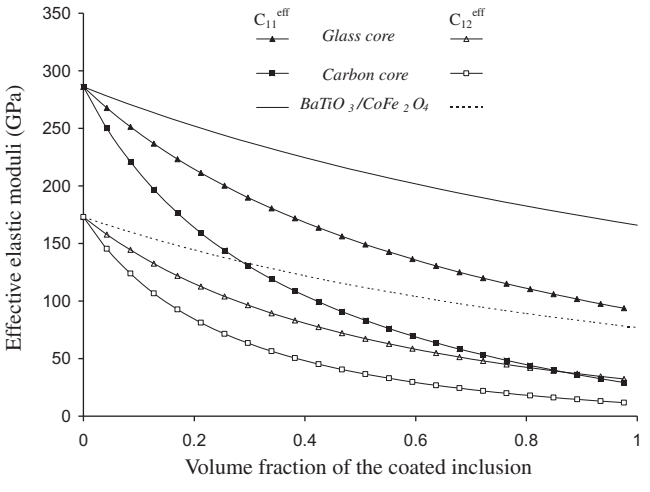

Fig. 7b. Effective elastic moduli C_{11}^{eff} and C_{12}^{eff} for $BaTiO_3$/$CoFe_2O_4$ fibrous composites and for hybrid composites reinforced by glassy or carbon core ($c/a = 100$ and $\Delta a/a = 0.02$).

4. Conclusions

We obtain the effective magneto-electro-elastic properties of a magnetic-piezoelectric composites reinforced by coated inclusions in the general case of anisotropic materials and ellipsoidal inclusions with non homothetic topology. Moreover, the solution of the magneto-electro-elastic coated inclusion problem is only based on the classical Eshelby's magneto-electro-elastic tensors.

The micromechanical model is applied to particular coated inclusions in magnetic matrix: piezoelectric layer surrounding a glassy core or a carbon core. Some comparisons with two phase models are successfully conducted. A potential enhancement of the magneto-electric coupling effects may be obtained provided that the shape, the thickness and orientation of the coated inclusion are thoughtfully chosen according to the direction to be optimized (poling or transverse). Lamellar shape induces higher ME coupling α_{11}^{eff} whereas cylindrical shape favors α_{33}^{eff}. For a given volume fraction of the coated inclusion, the ME coupling α_{33}^{eff} changes of sign for particular shapes. The increase of the thickness coating increases the ME coupling effects. The ME coupling effects α_{33}^{eff} are optimized for an orientation of the fibers of 45° with the poling direction. A more detailed study of the choice of the material core could also offer tracks of improvement. The present model may provide also homogenized properties indispensable to the optimization of the mechanical strength of the hybrid composite (elastic stiffness, piezoelectric and piezomagnetic properties, dielectric constants and magnetic permeabilities).

References

Alshits, V.L., Darinskii, A.N., Lothe, J., 1992. On the existence of surface waves in half-infinite anisotropic media with piezoelectric and piezomagnetic properties. Wave Motion 16, 265–285.

Benveniste, Y., 1995. Magnetoelectric effect in fibrous composites with piezoelectric and piezomagnetic phases. Phys. Rev. B 51 (22), 16424–16427.

Cherkaoui, M., Sabar, H., Berveiller, M., 1995. Elastic composites with coated reinforcements: a micromechanical approach for nonhomothetic topology. Int. J. Eng. Sci. 33 (6), 829–843.

Cherkaoui, M., Muller, D., Sabar, H., Berveiller, M., 1996. Thermoelastic behavior of composites with coated reinforcements: a micromechanical approach and applications. Comput. Mater. Sci. 5, 45–52.

Dinzart, F., Sabar, H., 2009. Electroelastic behavior of piezoelectric composites with coated reinforcements: micromechanical approach and applications. Int. J. Solid Struct. 46, 3556–3564.

Dunn, M.L., 1994. The effects of crack face boundary conditions on the fracture mechanics of piezoelectric ceramics. Eng. Fracture Mech. 48, 25–39.

Dunn, M.L., Taya, M., 1994. Electroelastic stress concentrations in and around inhomogeneities in piezoelectric solids. J. Appl. Mech. 61, 474–475.

Eshelby, J.D., 1957. The determination of the elastic field of an ellipsoidal inclusion, and related problems. Proc. R. Soc. Lond. A24, 376–396.

Harshe, G., Dougherty, J.P., Newnham, R.E., 1993. Theoretical modeling of multilayer magnetoelectric composites. Int. J. Appl. Electromagn. Mater. 4, 145–159.

Hill, R., 1983. Interfacial operators in the mechanics of composite media. J. Mech. Phys. Solids 31, 347–357.

Hori, M., Nemat-Nasser, S., 1993. Double-inclusion model and overall moduli of multi-phase composites. Mech. Mat. 14, 189–206.

Hu, G.K., Weng, G.J., 2000. The connections between the double-inclusion model and the Ponte Castaneda–Willis, Mori–Tanaka, and Kuster–Toksoz model. Mech. Mat. 32, 495–503.

Huang, J.H., Kuo, W.S., 1997. The analysis of piezoelectric/piezomagnetic composite materials containing ellipsoidal inclusions. J. Appl. Phys. 81 (3), 1378–1386.

Huang, J.K., Chiu, Y.H., Liu, H.K., 1998. Magneto-electro-elastic Eshelby tensors for a piezoelectric-piezomagnetic composite reinforced by ellipsoidal inclusion. J. Appl. Phys. 83, 5364–5370.

Huang, J., Liu, H., Dai, W., 2000. The optimized fiber volume fraction for magneto-electric coupling effect in piezoelectric-piezomagnetic continuous fiber reinforced composites. Int. J. Eng. Sci. 38, 1207–1217.

Islam, R.A., Bedekar, V., Poudyal, N., Liu, J.P., Priya, S., 2008. Magnetoelectric properties of core-shell particulate nanocomposites. J. Appl. Phys. 104, 104–111.

Jiang, C.P., Cheung, Y.K., 2001. An exact solution for the three-phase piezoelectric cylinder model under antiplane shear and its applications to piezoelectric composites. Int. J. Solid Struct. 38, 4777–4796.

Kari, S., Berger, H., Gabbert, U., Guinovart-Diaz, R., Bravo-Castillero, J., Roriguez-Ramos, R., 2008. Evaluation of influence of interphase material parameters on effective material properties of three phase composites. Compos. Sci. Technol. 68, 684–691.

Lee, J., Boyd, J.G., Lagoudas, D.C., 2005. Effective properties of three-phase electro-magneto-elastic composites. Int. J. Eng. Sci. 43, 790–825.

Li, J.Y., Dunn, M.L., 1998. Anisotropic coupled-field inclusion and inhomogeneity problems. Philos. Mag. A 77, 1341–1350.

Li, J.Y., 2000a. Magnetoelectroelastic multi-inclusion and inhomogeneity problems and their applications in composite materials. Int. J. Eng. Sci. 38, 1993–2011.

Li, J.Y., 2000b. Thermoelastic behavior of composites with functionally graded interphase: a multi-inclusion model. Int. J. Solid Struct. 38, 5579–5597.
Lin, Y., Sodano, H.A., 2010. A double inclusion model for multiphase piezoelectric composites. Smart Mater. Struct. 19 (035003), 0964–1726.
Liu, Y.X., Wan, J.G., Liu, J.M., Nan, C.W., 2003. Numerical modeling of magnetoelectric effect in composite structure. J. Appl. Phys. 94 (8), 5111–5117.
Mori, T., Tanaka, K., 1973. Average stress in matrix and average elastic energy of materials with misfitting inclusions. Acta Metall. 21, 571–574.
Mura, T., 1987. Micromechanics of defects in solids, second ed. Martinus Nijhoff, Dordrecht.
Nan, C.W., Bichurin, M.I., Dong, S., Viehland, D., Srinivasan, G., 2008. Multiferroic magnetoelectric composites: historical perspective, status, and future directions. J. Appl. Phys. 031101, 1–35.
Nye, J.F., 1957. Physical properties of crystals: their representation by tensors and matrix. Clarendon, Oxford.
Odegard, G.M., 2004. Constituve modeling of piezoelectric polymer composites. Acta Mater. 52, 5315–5330.
Sevostianov, I., Kachanov, M., 2007. Effect of interphase layers on the overall elastic and conductive properties of matrix composites. Applications to nanosize inclusion. Int. J. Solid Struct. 44, 1304–1315.
Shen, M.H., 2008. A magnetoelectric screw dislocation interacting with a circular layered inclusion. European J. Mech. A/ Solids 27, 429–442.
Srinivas, S., Li, J.Y., 2005. The effective magnetoelectric coefficients of polycrystalline multiferroic composites. Acta Materialia 53, 4135–4142.
Sudak, L.J., 2003. Effect of an interphase layer on the electroelastic stresses within a three-phase elliptic inclusion. Int. J. Eng. Sci. 41, 1019–1039.
Tang, T., Yu, W., 2008. Variational asymptotic homogenization of heterogeneous electromagnetoelastic materials. Int. J. Eng. Sci. 46, 741–757.
Tong, Z.H., Lo, S.H., Jiang, C.P., Cheung, Y.K., 2008. An exact solution for the three-phase thermo-electro-magneto-elastic cylinder model and its application to piezoelectric-magnetic fiber composites. Int. J. Solid Struct. 45, 5205–5219.
Torah, R.N., Beeby, S.P., White, N.M., 2004. Improving the electroelastic properties of thick-film PZT: the influence of paste composition, powder milling process and electrode material. Sensors Actuators A: Phys. 110, 378–384.
Xie, S.H., Li, J.Y., Qiao, Y., Liu, Y.Y., Nan, L.N., Zhou, Y.C., Tan, S.T., 2008. Multiferroic $CoFe_2O_4$ – $Pb(Zr_{0.52}Ti_{0.4})O_3$ nanofibers by electrospinning. Appl. Phys. Lett. 92, 062901.
Zhang, Z.K., Soh, A.K., 2005. Micromechanics predictions of the effective moduli of magnetoelectroelastic composite materials. European J. Mech. A/ Solids, 1054–1067.

Further reading

Saint-Gobain, <www.saint-gobainvetrotex.com>.